Int. J. Electrochem. Sci., 8 **(2013)** 2958 - 2967

International Journal of
ELECTROCHEMICAL
SCIENCE
www.electrochemsci.org

A Research of Intergranular Corrosion Sensitivity and Passive Film of Alloy 690

Wang Ju-lin[1], *Li Mo*[1], *Zheng Wen-jie*[2], *Qian Guang-ning*[1]

[1] College of Materials Science and Engineering Beijing University of Chemical Technology, Beijing 100029, PR China
[2] Research Institute of Functional Materials Central Iron & Steel Research Institute, Beijing 100081, PR China
*E-mail: julinwang@126.com

Received: 20 December 2012 / *Accepted:* 9 January 2013 / *Published:* 1 February 2013

The susceptibility to intergranular corrosion (IGC) in 2M H_2SO_4＋0.001M KSCN of alloy 690 under different thermal treatment (TT) has been investigated using double-loop electrochemical potentiokinetic reactivating (DL-EPR). The chemical composition and the semiconducting properties of passive films formed on alloy 690 in nitric acid were studied by using X-ray photoelectron spectrom (XPS) and the Mott-Schottky (M-S) analysis. The optimum heat treatment of resistant to IGC is solution treatment in 1090°C for 2min followed by the thermal treatment in 715°C for 10h. The M-S curves indicate the specimen has produced the n-type and the p-type semiconductor at 0.08V and 0.6V, respectively. And when the thermal-treatment temperature is higher than 715°C, they become denser. The reason is the passive films which produced in the HNO_3 solution is mainly chromium oxide, and as the raise of thermal treatment temperature, the content of iron oxide reduces rapidly, and leads to a compact passive film.

Keywords: Alloy 690, DL-EPR, Mott-Schottky plot, Intergranular corrosion (IGC), Passive film

1. INTRODUCTION

Recently, the nuclear power station accident caused huge losses. So the safety and stability of the nuclear power plant's operation has become research focus. Since the steam generator (SG) is the primary-level components of the nuclear power plant, the study on the corrosion resistance of the heat exchange tube has been focused on.

In the 1970s, the American developed alloy 690. Since then, owing to its good stress corrosion cracking (SCC) resistance in high temperature aqueous environments, 690 alloy have become the best material for nuclear steam generators (SG) tube[1-3].During the using of the SG tube, intergranular corrosion (IGC) and intergranular corrosion cracking may cause the consumption of the tube. So the IGC resistant of the SG tube is the significant research content of the recent study.

Double-loop electrochemical potentiokinetic reactivating tests (DL-EPR) [4] is a test method can provide a nondestructive means of quantifying the degree of sensitization. This test method has found wide acceptance in studies of the effects of sensitization on IGC and intergranular corrosion cracking behavior. During the test, the specimen immersed in acidic solution, so that it is activated at the corrosion potential state and then changed into passive state through the anodic polarization. Subsequently, the specimen was scanned from the cathode state toward the anode with a given rate. The polarization curves of the process are shown in Figure 1. The maximum anodic current density (I_a) and maximum reactivation current density (I_r) were measured from the forward and reverse scan curves, respectively. And define the I_r:I_a ratio R_a=I_r/I_a as the measurement of IGC.

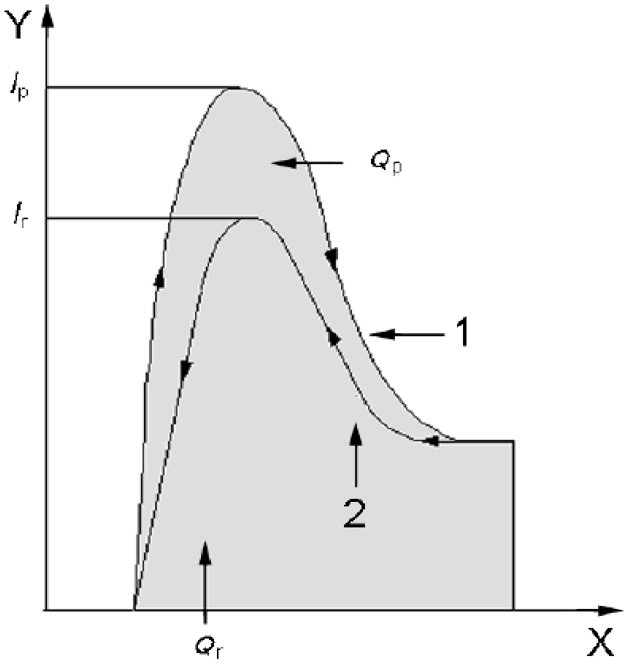

Figure 1. The sketch of polarization curve in double-loop EPR test method X-electric potential, Y-log current density, 1-anode scanning, 2-reactivation scanning.

The effects of thermal treatment on the resistance to IGC for Alloy 690 in 0.5M H_2SO_4+ 0.0001 M KSCN have been investigated by M.Casales [5], H.T.Lee [6], Z.G.Song [7] et al. in a DL-EPR method. R.S.Dutta [8] et al. have also reported by the similar research method to study the resistance of IGC of alloy 690 in 0.01 M H_2SO_4 + 10 ppm KSCN at the room temperature.

X-ray Photoelectron Spectroscopy (XPS) is one of the most widely used methods of surface analysis, mainly employed for composition and chemical state analysis. It can be used to investigat the chemical composition, the chemical states and the thickness of the surface oxide film which formed on the metal surface[9-14], and describe the oxide film as having a duplex structure formed by an inner

Cr-rich layer and an outer layer consisting of well-defined octahedral Ni-rich crystals (nickel alloys)[11].

M-S analysis has been employed to determine the semiconductor type and dopant density of the passive film. According to the liner parts of the curves, a negative slope means the p-type semiconducting behaviour and an n-type semiconducting behaviour with a positive slope. And the Fe oxides are the n-type semiconductor, while the Cr oxides are the p-type semiconductor [15].

During the semiconductor nature research of the nickel base alloy passive film, the measured capacitance is expected to be primarily caused by the space charge capacitance, C_{SC}, which is related to the applied electrode potential through the classical M-S relationship [16-17].

The equations for M-S analysis are:

$$\frac{1}{C_{SC}^2}=\frac{2}{\varepsilon\varepsilon_0 e N_D A^2}(E-E_{FB}-\frac{KT}{e}) \quad \text{n-type semiconductor} \qquad (1)$$

$$\frac{1}{C_{SC}^2}=\frac{2}{\varepsilon\varepsilon_0 e N_A A^2}(E-E_{FB}-\frac{KT}{e}) \quad \text{p-type semiconductor} \qquad (2)$$

Where ε_0 is the vacuum permittivity (8.85419×10^{-14}F/cm), $\varepsilon$is the dielectric constant of the passive film, N_D and N_A are the donor and acceptor densities (cm^{-3}), K is the Boltzmann constant (1.38×10^{-23} J/K), T is the absolute temperature and E_{FB} is the flat band potential (V), A is the area of the specimen (cm^2), e is the electron charge (1.602189×10^{-19}C).

C.T.Li [18-21] used M-S curves to study the effect of the pH value, chlorine ion and lead oxide on the electrochemical performance of 690 alloy passivated film. Accroding the investigation, 690 alloy had the obvious passivation interval in the acid medium, whereas when it was conducted in a alkali medium, passivated film was more dense and chloride ions increased the donor-acceptor pair density, thus reduced the protection of the film. And PbO has also reduced the film’s protection performance. Investigations carried out by T.C.Dan [22] observed the influence of hydrogen to 690 alloy anode behavior by using the M-S curve, which revealed that the hydrogen increased the donor-acceptor pair density, result in a poor protection of the TT surface of 690 alloy passivated film.

2. MATERIALS AND METHODS

2.1 Test material and sample preparation

Table 1. Chemical composition of the alloy 690 specimen (wt.%).

Elements	Ni	Cr	Fe	Mn	Si	Ti	Al	C
wt.%	Bal.	29.42	9.10	0.32	0.30	0.26	0.16	0.015

Table 2. The Numbers and the thermal treatment of the samples

No.	Thermal treatment
MWW1	1090°C×2min + 650°C×10h
MWW2	1090°C×2min + 700°C×10h
MWW3	1090°C×2min + 715°C×10h
MWW4	1090°C×2min + 725°C×10h
MWW5	1090°C×2min + 750°C×10h
MWW6	1090°C×2min + 780°C×10h
MWW7	1090°C×2min + 800°C×10h
MWW8	1090°C×2min + 850°C×10h

All the samples are own developed 690 alloy by the method of vacuum induction melting (VIM) and electroslag remelting (ESR). And the chemical composition of the alloy 690 specimen is presented in Table 1. After the forging, hot rolling and then cold rolled into 1 mm thick plate, the samples were under thermal treatment in accordance with the Table 2, and then cut into square specimens of 10.5mm ×10.5mm through linear cutting.

2.2 Electrochemical measurements

All electrochemical tests were performed using a three-electrode cell system consisting of a saturated calomel electrode (SCE) as a reference, a platinum electrode as a counter, and a specimen as a working electrode.

Before the experiment, the test specimens were polished with silicon papers up to 400# grit. Then the specimens were welded to copper wires and measured the working surface area, finally sealed with the epoxy resin. The test specimen working surface were gradually polished with silicon papers up to 2000# and kept immersed in the test solution for more than 30 min at open-circuit potential, and the 200ml test solution was purged with high purity N_2 gas to remove dissolved oxygen from the aqueous solution before and during each test.

2.2.1 The DL-EPR test

The effect of different thermal treatments on the resistance to IGC was evaluated by the double-loop electrochemical potentiokinetic reactivation (DL-EPR) test in 2M H_2SO_4 + 0.001M KSCN at 50°C. With a scanning rate of 1.67mV/s, when the potential reached in +200 mV_{SCE}, constant potential polarization would be employed in that potential with 2 min, then scanning reverse with same rate and finally reduced to E_{corr}. The maximum anodic current density (I_a) and maximum reactivation current density (I_r) were measured from the forward and reverse scan curves, respectively. And define the I_r:I_a ratio as the measurement of IGC.

2.2.2 Mott-Schottky analysis

Passive films were prepared by holding at $0.1V_{SCE}$ for 1 h in the 35% HNO_3 by conducted constant potential polarization [21]. The capacitance measurements were performed in 2M H_2SO_4 + 0.001M KSCN at 50°C, under a frequency of 1 kHz and made at 0.02V intervals in the potential range from -1.0 to 1.0 V with the disturbance potential of 10mV.

2.3 X-ray Photoelectron Spectrom (XPS) analysis

Surface analyses by XPS were conducted for the specimens which were gradually polished with silicon papers up to 2000# grit, then passivated in the 35% HNO_3 at 30ºC for 6h. The X-ray source was AlKα, monochromator and operated at 500W. The energy of the high resolution scanning was 30eV, and the test area was $500\mu m^2$.

3. RESULTS AND DISCUSSION

3.1 Electrochemical behavior (*DL-EPR)*

Figure 2 shows the DL-EPR curves, Table 3 lists the R_a value and Figure 3 reveals the relationship between R_a value and the TT temperature.

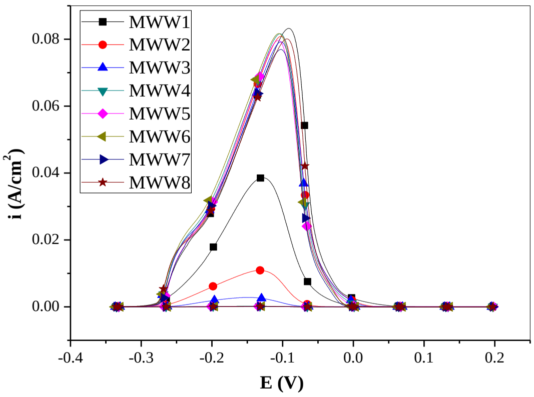

Figure 2. The DL-EPR test curves of alloy 690 with different thermal treatments.

Table 3. The R_a values of alloy 690 with different thermal treatments.

No.	MWW1	MWW2	MWW3	MWW4	MWW5	MWW6	MWW7	MWW8
Ra (%)	47.29	12.85	2.56	0.31	0.21	0.15	0.14	0.15

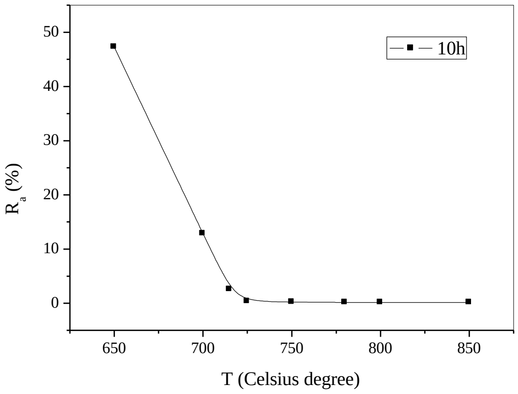

Figure 3. The relationship between R_a value and the TT temperature for alloy 690.

Obviously, sharp drop of the R_a ratio reveals the resistance of IGC rapidly increases with the thermal-treatment temperature raise till reaches up to 715ºC. When the thermal-treatment temperature is higher than 715ºC, the R_a ratio is almost invariable, and maintains at a very low level, shows the test specimen has a good resistance of IGC.

3.2 XPS results

The composition and structure of passive film formed on Alloy 690 in nitric acid were investigated by X-ray photoelectron spectroscopy (XPS). The passive film was mainly composed of O, Cr, Ni and Fe. Figure 4-6 show the binding energy photoelectron spectra of the element Cr, Fe, Ni in the specimen surface, respectively. And the surface elements and content of the specimen are presented in Table 4 and the binding energy of photoelectrons of specimen surface is given in Table 5.

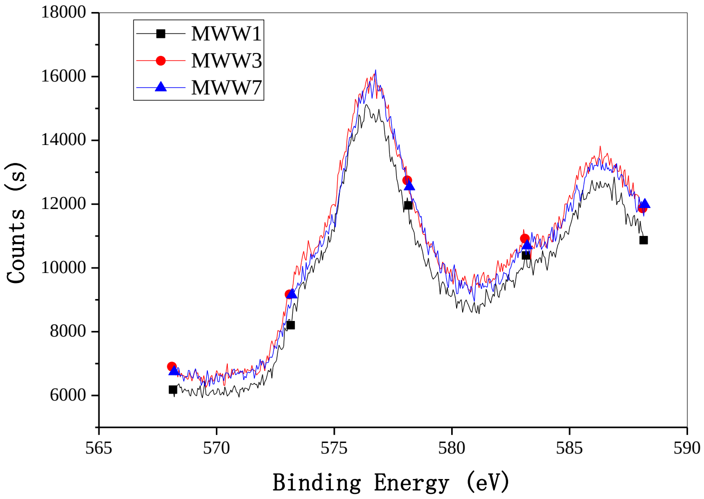

Figure 4. The photoelectron binding energy spectrogram of Cr in the specimen surface.

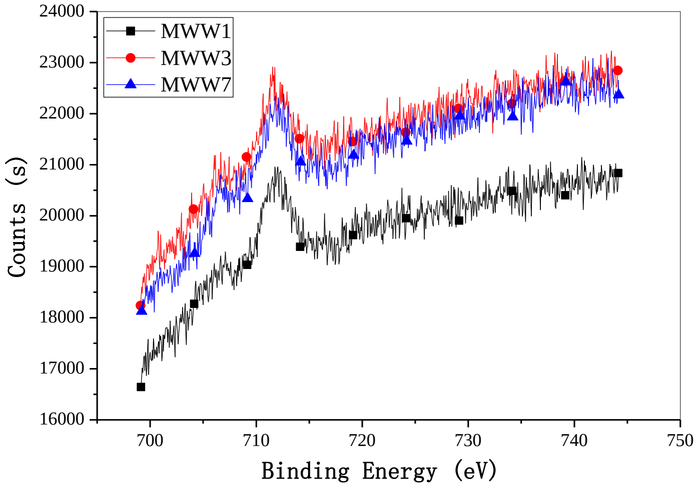

Figure 5. The photoelectron binding energy spectrogram of Fe in the specimen surface.

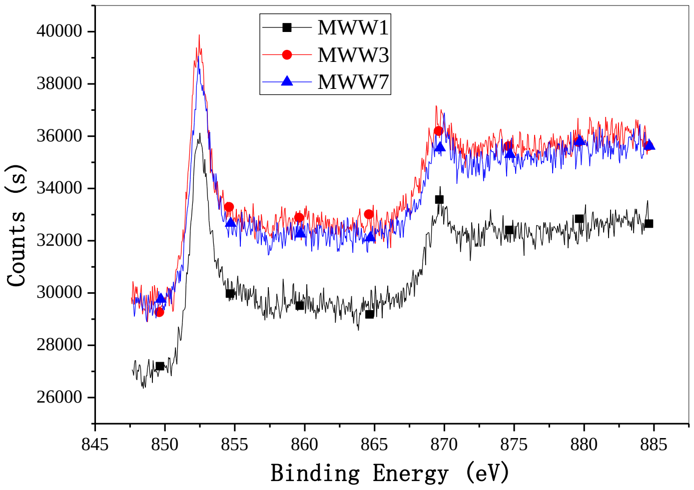

Figure 6. The photoelectron binding energy spectrogram of Ni in the specimen surface.

Table 4. Specimen surface elements and content (At%)

No.	Cr	Fe	Ni	O
MWW1	11.25	1.65	3.31	38.64
MWW3	11.50	0.76	3.03	37.59
MWW7	11.31	0.53	3.41	35.87

Table 5. The photoelectron binding energy (eV) of the element in the specimen surface.

No.	Cr	Fe	Ni
MWW1	576.35	711.80	852.50
MWW3	576.70	711.55	852.45
MWW7	576.75	711.80	852.50
N13	576.75	706.86	852.60

Consult PHI 5300 ESCA databases to obtain the consequences follow from this: Cr_2O_3, 576.80eV; CrO_2, 576.30 eV; Fe,706.74,706.82,706.98 eV; γ-FeOOH, 711.30 eV; α-FeOOH, 711.80 eV; Ni, 852.65,852.68,852.73,852.80(15) eV. So the composition of the surface on MWW1 was CrO_2, few α-FeOOH and Ni. The MWW3 was Cr_2O_3, few γ-FeOOH and Ni, while the MWW7 was Cr_2O_3, few α-FeOOH and Ni.

And with the increase of TT temperature from 650°C to 700°C and then 715°C, the content of the Fe oxide, which has a poor protective effect in the passive film, quickly reduces. While the content of Cr oxide, which perform a better protective effect, increases slightly and become more dense from CrO_2 to Cr_2O_3. As a result the resistance of IGC is enhanced.

3.3 Mott–Schottky plots

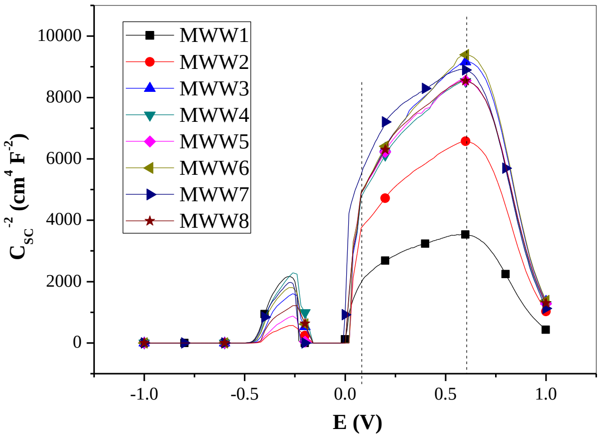

Figure 7. The Mott–Schottky plots of alloy 690 with different thermal treatments.

Figure 7 shows the Mott–Schottky cruves of the different thermal-treatment temperatures of Alloy 690, the plot of C_{SC}^{-2} vs. the applied potential E which have two peaks between -0.5V to -0.24V, 0.08V to 0.6V respectively. The former reveals the remove of the pre-passivation film, which produced in the nitric acid, during the cathode polarization in 2 M H_2SO_4+0.001 M KSCN. While the latter indicates the production of the passivation film in 2 M H_2SO_4+0.001 M the KSCN during the anodic polarization. And the same peak type shows the similarity of the two passivation films. In order to concise, the anodic polarization cruves was discussed.

The cruves, which range from 0.0V to 1.0V, indicated the existence of three regions where Mott–Schottky behaviours could be observed (straight lines below 0.08V, 0.08V - 0.60V and above 0.60V). With the two linear positive slopes and a negative one, the structure of the passivation film which was formed in 2 M H_2SO_4+0.001 M KSCN was a two-level structure demonstrated the iron oxides and chromium oxides, respectively[15]. The switch potentials in slope were 0.08V and 0.60V.

Both the slopes of 0-0.08V and 0.08V-0.60V are positive, which show that the passivation films are n-type semiconductor namely iron oxide film, but the latter is smaller than the former.

Acrroding to the equation (1), the slope is proportional to 1/ N_D. As to the intergranular corrosion damage for alloy 690, the passive film will be destroyed firstly, and then goes deep into the grain boundary. So the high doping densities (N_D), which causes the unstable passive films, leads to the poor protection to the matrix. That is to say that the former passivation films, which have the more positive slopes, present more stable and show a better protection performance.

With the increasing temperature of the thermal-treatment, the slopes between 0-0.6V become more positive, respectively. And when the temperature reached more than 715°C, the slopes were remained steady. It revealed that increasing the temperature of the heat treatment could lead to a dense passivation film, and give a good resisitance of IGC to the samples. Then the DL-EPR test gave the same conclusions.

Combined with the X-ray photoelectron spectroscopy (XPS) analysis on the results of passivation film, the more stable α-FeOOH passivation film would form when the potential at 0-0.08V. However, when at 0.08V-0.60V an unstable γ-FeOOH film might generate. Cr_2O_3 or CrO_2 films would form above 0.60V which were the most compact passive film and had a best protection of the matrix.

4. CONCLUSION

In the range from 650°C to 850°C in our research, the resisitance of IGC was affected on the thermal-treatment temperature of Alloy 690. It rapidly increased with the thermal-treatment temperature raise till the temperature reached 715°C. With the raise of thermal-treatment temperature, the passivation film became dense, leads to the stronger resistance to IGC. When the temperature reaches 715°C, the surface film was essentially unchanged and kept an excellent resistance to IGC. So when the thermal-treatment temperature is higher than 715°C, the test specimens presented a good resisitance of IGC and slightly improved with the increased temperature.

The structure of the passivation film formed in 2 M H_2SO_4+0.001 M KSCN was a two-level structure demonstrated the iron oxides and chromium oxides, respectively. And according to the Mott–Schottky plot, the switch potentials in slope were 0.08Vand 0.60V. When the potential was at 0-0.08V, the more stable α-FeOOH passivation film would form. However, when at 0.08V-0.60V an unstable γ-FeOOH film might generate. The most compact passive film namely Cr_2O_3 or CrO_2 films would form above 0.60V. And the passive films which produced in the HNO_3 solution are mainly chromium oxide, and with the raise of thermal treatment temperature, the content of iron oxide decline rapidly, and lead to a compact passive film.

References

1. G.S.Was, *Corros. Sci.*, 46 (1990) 319.
2. S.Xia, H.Li, T.G.Liu, B.X.Zhou, *J. Nucl. Mater.*, 416 (2011) 303–310.
3. B.Peng, B.T.Lu, J.L.Luo, Y.C.Lu, H.Y.Ma, *J. Nucl. Mater.*, 378 (2008) 333–340.
4. ASTM G108-94 (2010).
5. M.Casales, V.M.Salinas-Bravo, A.Martinez-Villafan, J.G. Gonzalez-Rodriguez, *Mater. Sci. Eng.*, A, 332 (2002) 223-230.
6. H.T.Lee, J.L.Wu, *Corros. Sci.*, 52 (2010) 1545-1550.

7. Z.G.Song, H.Feng, W.J.Zhen, *Journal of Iron and Steel Research (in Chinese)*, 22 (2010) 32-36.
8. R.S.Dutta, R.Tewari, P.K. De, *Corros. Sci*., 49 (2007) 303-318.
9. P.Ghodsa, O.B.Isgor, J.R.Brown, F.Bensebaa, D.Kingston, *Appl. Surf. Sci*., 257 (2011) 4669-4677.
10. D.Shintani, T.Ishida, H.Izumi, T.Fukutsuka, Y.Matsuo, Y.Sugie, *Corros. Sci.*, 50 (2008) 2840-2845.
11. A.Machet, A.Galtayries, S.Zanna, L.Klein, V.Maurice, P.Jolivet, M.Foucault, P.Combradec, P.Scott, P.Marcus, *Electrochim. Acta*, 49 (2004) 3957-3964.
12. I.Betova, M.Bojinov, V.Karastoyanov, P.Kinnunen, T.Saario, *Corros. Sci*., 58 (2012) 20-32.
13. F.Huang, J.Q.Wang, E.H.Han and W.Ke, *J. Mater. Sci. Technol*., 28 (2012) 562-568.
14. T.C.Dan, T.Shoji, Z.P.Lu, K.Sakaguchi, J.Q.Wang, E.H.Han, W.Ke, *Corros. Sci.*， 52 (2010) 1228-1236.
15. N.E.Hakiki, M.F.Montemor, M.G.S, *Corros. Sci*., 42 (2000) 687-702.
16. V.A.Alves, M.A.BrettC, *Electrochim. Acta*, 47 (2002) 2081-2091.
17. J.Sikora, E.Sikora, D.D.Macdonald, *Electrochim. Acta*, 45 (2000) 1875-1883.
18. C.T. Li, X.Q.Cheng, C.F.Dong, X.G.Li, *Mater. Prot*., 43 (2010) 4-7.
19. C.T. Li, X.Q.Cheng, C.F.Dong, X.G.Li, *Journal of Beijing Science and Technology University (in Chinese)*, 33 (2011) 444-448.
20. C.T. Li, X.Q.Cheng, C.F.Dong, X.G.Li, *Corrosion and Protection (in Chinese)*, 32 (2011) 252-255.
21. C.T. Li, X.Q.Cheng, C.F.Dong Z.J.Jia, X.G.Li, *Acta Metall. Sin*, 23 (2010) 343-350.
22. J.Q.Wang, W.H.Wu, M.C.Feng, *Electronic Spectroscopy Introduction (in Chinese)*, National Defense Industry press, Beijing (1992).